Electrical lithium battery performance model for second life applications

Edoardo Locorotondo
DIEF
University of Florence
Florence, Italy
edoardo.locorotondo@unifi.it

Vincenzo Cultrera
DINFO
University of Florence
Florence, Italy
vincenzo.cultrera@unifi.it

Luca Pugi
DIEF
University of Florence
Florence, Italy
luca.pugi@unifi.it

Lorenzo Berzi
DIEF
University of Florence
Florence, Italy
lorenzo.berzi@unifi.it

Manlio Pasquali
ENEA
Centro Ricerca ENEA
Rome, Italy
manlio.pasquali@enea.it

Natascia Andrenacci
ENEA
Centro Ricerca ENEA
Rome, Italy
natascia.andrenacci@enea.it

Giovanni Lutzemberger
DESTEC
University of Pisa
Pisa, Italy
lutzemberger@dsea.unipi.it

Marco Pierini
DIEF
University of Florence
Florence, Italy
marco.pierini@unifi.it

***Abstract*— The aging behavior of lithium cell has a profound impact on its performance in terms of energy and power efficiency, especially when it is considered in End Of Life (EOL) in automotive field. Lithium battery is considered in EOL if at 85-80% of nominal capacity. Today, the reusing of Electric and Hybrid Vehicles EOL batteries on stationary applications, giving a second life to these batteries, is a solution to reduce high potential cost of lithium batteries. Currently, there is a lack of investigation of the performances of these second life batteries. This paper depicts the performance results of five NMC cells at different SOH, where four of these cells are considered in EOL, so ready to be investigated for possible second use. By results, there are many way to correlate battery SOH and battery performance, e.g. an increase of the internal resistance and the constant-voltage (CV) phase charging duration, the change of the open circuit voltage shape curve. Finally, a battery model based on electrical equivalent circuit is build and implemented in Matlab/Simulink, which is validated by comparison between voltage experimental and simulated data.**

Keywords*— *Lithium cell, Electrical Equivalent Circuit, State of health, Second life battery, grid connected energy storage applications, State of Charge, Aging.

I. INTRODUCTION

When it comes to the impact Electric Vehicles (EVs) have on society, we know that they are important to contribute towards stopping the global warming and reduce both emissions and environmental pollution. Currently, a quarter of the greenhouse relevant CO_2 emissions are caused by transport and about 40% by electricity grid [1]. Thus, the development of electrical mobility systems is a fundamental topic for European research project. In particular, the management and monitoring of energy accumulators in EVs are one of the main topics. The current dominant technology deployed for electric traction batteries is lithium-ion [2], due to high power and energy capability, high efficiency, long cycle and calendar life. This, in turn, has led to rapidly increasing demand for lithium battery in automotive field. This will also translate into an increase of exhausted Electric Vehicle Batteries (EVBs) after reaching the End of Life (EOL). EVB is considered in EOL if its current capacity is at 85-80% of nominal capacity. Among several solutions, as recycling, their residual capacity could be used in other applications before recycling, giving them a "Second Life" [3]. EVB in second life could be used as energy storage, satisfying the requirements of stationary applications, which require low performance. A second life Battery Energy Storage System (BESS) combined with renewable energy sources (from wind and solar), should support electrical grid, e.g. supplying the evening peak demand [4]. Today, car manufacturers are using the second life option in an attempt to expand their portfolio and enter in the stationary battery market. In cooperation with utility companies, they are launching several battery second life pilot projects. Summary of these projects is presented in [5]. Assuming that second life lithium battery can be used, an electronic control unit should be employed in BESS in order to enhance its performance and ensure safety and long lifetime. In literature, this control unit is called Battery Management System (BMS). Monitoring and management of lithium-ion second life battery is the topic on this paper. To improve battery state estimation, BMS should be able to simulate its electric behavior, like voltage, during the charge and discharge processes using a mathematical model. This consideration is more important if the battery state estimation, based on estimators as State of Charge (SOC) [6], State of Health (SOH) [7], internal temperature [8], is carried out by using model-base observers, e.g. Kalman filter [9] or sliding mode [10] approach. Thus, battery model is usually employed on BMS. Currently, battery models have been well studied by many authors in literature, concerning battery state evolution [11], or comparing model complexity and accuracy [12]. Nevertheless, there is a lack of investigation of the performances of the second life batteries, and of second life

This project has received funding from the European Union's Horizon 2020 research and innovation program under grant agreement No 769506.

978-1-7281-7455-6/20/$31.00 ©2020 IEEE

battery models for simulations. The scope of this paper is to provide more information as possible about battery performance after EOL, analyzing strengths and weaknesses during charge and discharge phase. To achieve this scope, a battery virtual model is realized and implemented in Matlab/Simulink. The battery model is based on an electrical equivalent Thevenin circuit, which parameters are extracted by an appropriate parameter identification algorithm, test procedure and experimental data of five Li-Ion Nickel-Manganese-Cobalt (NMC) cells at different SOH. The effectiveness of the model accuracy is evaluated by comparison between experimental data and simulation results.

II. BATTERY MODEL

A. Electrical Equivalent Circuit (EEC) battery model based

A large number of battery models have been developed in literature. Despite electrochemical models, that simulate the internal dynamics of the lithium cells [13], present optimal model accuracy, these models are computationally-intensive and unsuitable for real time application. Instead, correlating the electrochemical battery properties to circuit elements, so realizing an electrical lumped parameters model based on equivalent circuit, model complexity is reduced. In literature, these models are so-called Electrical Equivalent Circuit battery models [14][15], and are typically used because solve the trade-off between model accuracy and complexity. The general structure is depicted in Fig.1. Giving an input current, is possible to describe battery voltage behavior by differential equations. Battery voltage V_{batt} is represented by an equivalent Thevenin circuit, in which the Open Circuit Voltage (OCV), represented by an ideal voltage generator, is in series to a static resistance R_{int}, which defines the battery internal resistance, and, finally, an appropriate number of RC blocks, which corresponds to battery voltage relaxation [16]. Usually, no more than two RC blocks are adopted for real time application and battery model simulations. As depicted in Fig.1, voltage V_{batt} is calculated by the differential system equation (1), where $\tau_i = R_i C_i$:

$$\begin{cases} \dot{v}_1(t) = \dfrac{v_1(t)}{\tau_1} - \dfrac{i_{batt}(t)}{C_1} \\ \dot{v}_2(t) = +\dfrac{v_2(t)}{\tau_2} - \dfrac{i_{batt}(t)}{C_2} \\ V_{batt} = OCV - v_1(t) - v_2(t) - R_{\text{int}} i_{batt}(t) \end{cases} \quad (1)$$

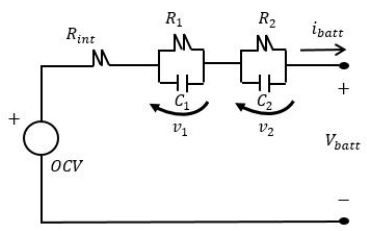

Fig. 1. Battery performance model based on Electrical Equivalent Circuit (EEC).

B. Non-linear and Time-Varying battery dynamic system

Battery model considered in (1) could be classified as a linear and time-invariant dynamic system. However, an accurate battery model should have several non-linear properties. Indeed, the OCV is related with SOC by non-linear features, having a flat portion in the middle of SOC window, and exponential trend at its extreme parts at the extreme of SOC window in lithium batteries as LiFePO4 [14], NMC[15], NCA[17] types. Moreover, in [16] it is noticeable the OCV difference between charging and discharging curves, due to the hysteresis behavior which battery has, especially for LiFePO4 cathode type. Finally, battery aging process impacts on OCV [18]. Concerning circuit elements in (2) like R_{int}, R_1, R_2, C_1, C_2, their values change at different SOC [14], temperature [19] and aging process [7]. Considering these assumptions, a more accurate battery model is based on (2):

$$\begin{cases} \dot{v}_1(t) = \dfrac{v_1(t)}{\tau_1} - \dfrac{i_{batt}(t)}{C_1} \\ \dot{v}_2(t) = \dfrac{v_2(t)}{\tau_2} - \dfrac{i_{batt}(t)}{C_2} \\ OCV(t) = g(SOC(t), SOH, sign(i_{batt}(t))) \\ Z_{batt}(t) = f(SOC(t), SOH, sign(i_{batt}(t))) \\ V_{batt} = OCV(t) - v_1(t) - v_2(t) - R_{\text{int}} i_{batt}(t) \end{cases} \quad (2)$$

Where Z_{batt} is the impedance vector, which its parameters [R_{int}, R_1, R_2, C_1, C_2] and OCV depend respectively by analytical vector function f and g and variables SOC, charging and discharging phase $sign(i_{batt}(t))$ and battery SOH. The state of charge SOC corresponds to the ratio of the stored battery capacity (the cumulate current supplied/delivered by the battery) with respect to the nominal current battery capacity (C_{curr}), in according to (3):

$$SOC(t) = SOC(0) - \left[\frac{1}{3600 C_{curr}} \int_0^t i_{batt}(\sigma) d\sigma \right] \times 100 \quad (3)$$

The state of health SOH considers the battery performance degradation over time due unexpected events, always by considering variation in battery capacity or internal resistance. In this paper, SOH value is based on a comparison of the current capacity evaluated with a standard cycle (C_{curr}) with the nominal capacity at the beginning of life (C_{nom}), in according to (4):

$$SOH = \frac{C_{curr}}{C_{nom}} \times 100 \quad (4)$$

Thus, battery model considered in (2) is classified as non-linear and time-varying dynamic system. Based on (2), in the next sections a standard characterization test procedure and mathematical method will be defined for model parameters evaluation.

III. CHARACTERIZATION TEST PROCEDURE

A. Battery cell under test

The battery cell under test is a Li-Ion NMC Cathode pouch cell type, having a nominal capacity of 20 Ah. The performance test are performed on five cells of the same manufacturer, but at different State of Health (SOH). One of this five cell is considered as new (cell #0, fresh cell); the other four cells have been cycled until they have reached EOL. The EOL cells (#3-#8) were subjected to 4 different cycle life test, composed by constant-current (CC) and, finally, constant-voltage (CV) charging (0.5C, where C is nominal capacity); followed by discharging phases, interspersed with pauses, at a room temperature of 35°C [20]. A summary of these cycle life test is presented in Table I. Cycle life tests were carried out in ENEA research center [20] from 2015 to 2017. More details about these tests are shown in [20][21]. Afterwards, the cells have not been used for about 2 years, and have been storage in the same conditions (in a not thermally controlled environment).

TABLE I. CYCLE LIFE TEST

Battery no.	Discharge C-Rate	Depth of Discharge	Performed cycle number	Last capacity estimated
#3	3	80-20%	2550	15.14 Ah
#4	5	80-20%	2000	15.09 Ah
#5	1	90-10%	2400	12.91 Ah
#8	3	90-10%	1600	15.48 Ah

B. Laboratory test setup

The experimental test setup is shown in Fig.2. The cell under test is excited under an appropriate current profile, generated by the Rigol DL3021 electronic load in discharging phase, and by the DSC Electronics DP15-60H in charging phase. Battery current, voltage, surface temperature and surrounding temperature are acquired by the DSpace MicroLabBox DS1202 at the following sample time: 0.1s for voltage and current measurement and 60s for temperature. DSpace device saves measurement data and manages the charging and discharging circuit, controlled by Host PC via Ethernet, through a software developed in Matlab/Simulink.

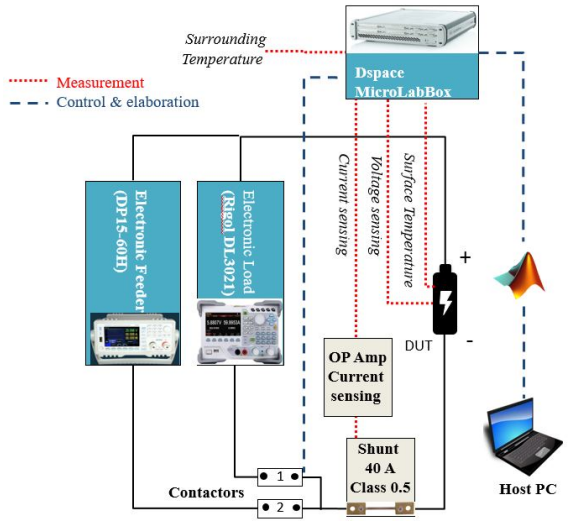

Fig. 2. Laboratory test & measurement setup

C. Test methodology

The battery cells are characterized by a set of subsequent performance tests, which aim to collect the necessary data to parametrize the battery EEC model described in (2). In the following, authors consider C-Rate current value referring at the maximum available cell capacity in the EOL state. This assumption is taken because second life applications, as shown in [3],[4], require low discharging current performance, in order to maintain a long service time of battery after their first life. Since the cells in EOL show different capacity values, as shown in Table I, every battery is excited with a different current amplitude. The following tests are performed on every battery:

- **Preconditioning Test:** is made up by three full discharge/charge cycles at fixed current amplitude of 4A, interspersed with a pause of 1h between discharging and charging phase. A 14h rest is undertaken that cycle is completed. By preconditioning test results, battery capacity is approximately calculated. In the following test, C-Rate is referred to the last capacity.
- **Capacity Test:** In order to evaluate battery capacity and coulombic efficiency, this test is made up by three full discharge/charge cycles, maintaining a charging C-Rate of C/3 (first in CC mode, finally in CV mode), changing the discharge C-Rate of C/2, C/3 and C/4. This is because battery capacity extracted during discharging phase depends on the current amplitude [14]. Rest time values are equals to preconditioning test.
- **Pulse Test:** When the battery is fully charged, it is excited by a series of fourteen C/2 discharged current pulses, separated by 30min of rest period. Each pulse discharges the 7% of battery capacity, until the lower threshold voltage is reached (3.0V). Then, after a rest of 14h, pulse charging test is performed, which is set as discharge pulse test, reaching the higher threshold voltage (4.15V) in CV mode. These tests are so important for battery impedance parameter Z_{batt} extraction. The identification method is illustrated in the next section.

D. Model parameters extraction

The model parameters extraction are based on experimental data obtained during the test, using appropriate mathematical methods. As mentioned before, model parameter values depend on SOC, temperature and aging process. Based on (2), model parameters will be considered having only a SOC and aging dependency.

The first extracted parameter is the battery capacity C_{curr}, obtained during capacity test. Using an Ampere-count method, battery capacity C_{curr} is in according to (5), calculating the integral of battery current during the test. The capacity is separately evaluated in charging or in discharging phase:

$$C_{curr} = \frac{1}{3600}\int i(\sigma)d\sigma \qquad (5)$$

The second extracted parameter is the OCV, obtained as the last voltage value acquired during voltage relaxation in the pulse test, see Fig.3. In this paper, the rest period, i.e. the voltage relaxation period between pulses, is 30 min. The internal resistance parameter R_{int} is acquired from the sudden drop voltage $V_{batt,drop}$ due to current pulse i_{pulse}:

$$R_{\text{int}} = \frac{V_{batt,drop}}{i_{pulse}} \tag{6}$$

Finally, last parameters R_1, R_2, C_1, C_2 are obtained in order to fit the voltage relaxation curve during the rest period, recalling the model (2) and Fig.3:

$$OCV - V_{batt}(t) = v_{1,drop} e^{-t/\tau_1} + v_{2,drop} e^{-t/\tau_2} \tag{7}$$

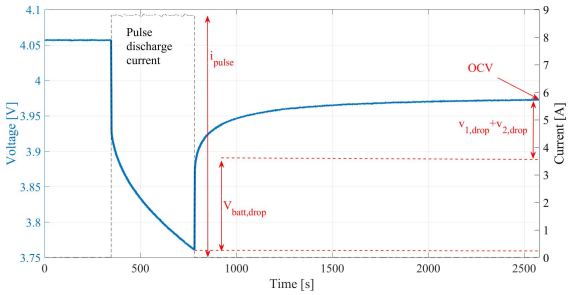

Fig. 3. Example of discharging pulse test.

The fitting process is carried out in Matlab software, using the curve fitting toolbox, where parameters $v_{1,drop}$, $v_{2,drop}$, τ_1, τ_2, are extracted using the bounded-parameter Trust-Region algorithm. Finally, R_1, R_2, C_1, C_2 parameters are calculated in according to (8)-(9):

$$R_i = \frac{v_{i,drop}}{i_{pulse}} \tag{8}$$

$$C_i = \frac{v_{i,drop}}{i_{pulse}} \tag{9}$$

IV. Results and Discussion

Test procedure, mentioned before, was performed on the five cells under test (#0 fresh cell, #3 SOH=80%, #4 SOH=85%, #5 SOH=60%, #8 SOH=50%), which SOH, in this paper, is considered as the ratio between the current battery maximum capacity and battery nominal capacity, evaluated during preconditioning test. All the tests were carried out in a not thermally controlled environment: measuring the room temperature, the mean and the maximum value obtained are respectively 22°C and 24°C. Concerning cell surface temperature, maximum temperature observed during the tests is 27°C.

A. Capacity test results

Three capacity test were performed on each five cells, with a discharging C-Rate respectively C/4, C/3, C/2, 1h of rest period and CC charging with C/3, followed by CV charging, as illustrated in Fig.4. The capacity test cycles have been exploited in order to observe the evolution of the voltage vs. charge/discharge on the five cells with different SOH. From results shown in Fig.5, two important points are highlighted. Firstly, it is noticeable a rise with aging of the CV charging phase duration, comparing the fresh cell (lower CV phase) with cell #3-#5 (higher CV phase) and cell#8 (highest CV phase duration), in according to results shown in [18] for NMC chemistries. Secondly, an increase with aging of the difference between voltage charging and discharging phase curves, due to an increase of the internal resistance with aging, as shown in Fig.10.

Finally, results of the battery coulombic efficiency are calculated and shown in Table II, in according to (10):

$$\eta = \frac{C_{curr,discharge}}{C_{curr,charge}} \tag{10}$$

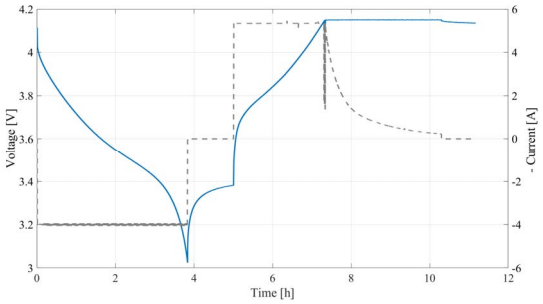

Fig. 4. Capacity test performed on cell #3 with C/4 of discharging current, and C/3 on charging current.

As mentioned before, authors consider C-Rate current value referring at the maximum available cell capacity in the current state, as estimated during the preconditioning test. Results depicted in Table II confirm that the coulombic efficiency of EOL cells, respect to the fresh cell, strongly decrease when battery discharge C-Rate increases.

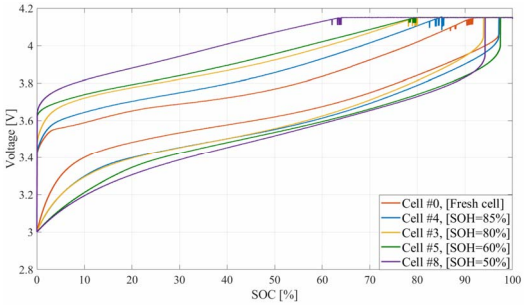

Fig. 5. Voltage vs. capacity for NMC cell at several SOH during charging and discharging phase.

TABLE II. CAPACITY TEST: AH EXTRACTED IN DISCHARGING PHASE AND COULOMBIC EFFICIENCY

n.	Charge Capacity	Capacity C/2 Test		Capacity C/3 Test		Capacity C/4 Test	
	[Ah]	[Ah]	η [%]	[Ah]	η [%]	[Ah]	η [%]
#0	18.15	17.61	97.0	17.64	97.2	17.95	98.9
#3	16.07	14.71	92.5	15.09	93.9	15.96	99.3
#4	17.14	15.40	89.9	16.65	97.1	16.90	98.6
#5	12.38	11.55	93.3	11.85	95.7	12.34	99.7
#8	10.60	8.84	83.4	9.99	94.3	10.28	97.0

B. *Pulse test results & model validation*

Pulse charge and discharge tests were performed, following the procedure illustrated in the previous section. These tests have been exploited in order to extract the impedance Z_{batt} and OCV parameters of the battery model (3), building and implementing the model in Matlab/Simulink and finally validating the model accuracy, by the comparison between voltage simulated and experimental data. Fig.6,8 show respectively the pulse charge/discharge test on cell #4. The voltage absolute error is shown in Fig. 7,9, defined as the difference between the measured and the simulated voltage.

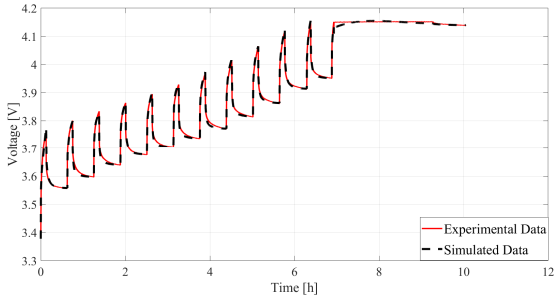

Fig. 6. Comparison between voltage measured and simulated data during the Pulse charge test performed on the cell #4.

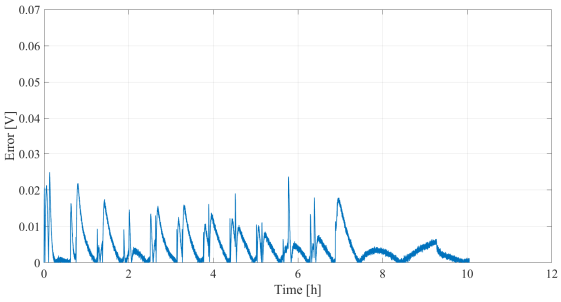

Fig. 7. Absolute error between voltage measured and simulated data during the Pulse charge test performed on the cell #4.

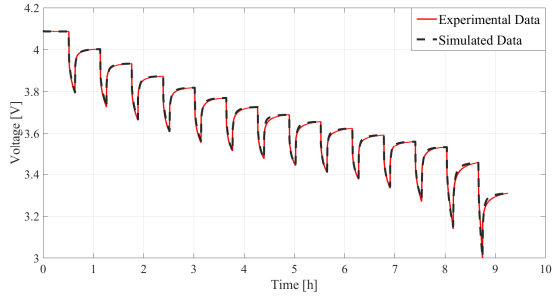

Fig. 8. Comparison between voltage measured and simulated data during the Pulse discharge test performed on the cell #4.

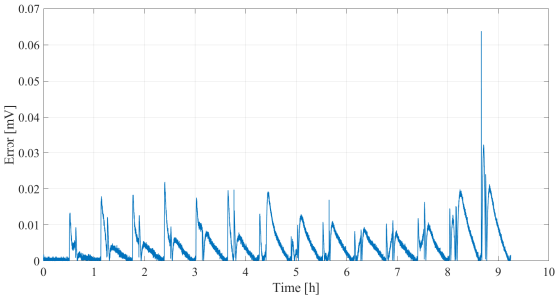

Fig. 9. Absolute error between voltage measured and simulated data during the Pulse discharge test performed on the cell #4.

Results shown in Fig.6-9 indicate that the battery model describes accurately the voltage evolution when the battery SOC is in the range [10,90]%, instead, at the extreme of battery SOC, so, when battery assumes non-linear behavior, the absolute error increases, especially at lowest SOC values. Finally, the effectiveness of battery model is performed on the comparison between experimental and simulation data based on the pulse charge/discharge test carried out on the five cells. The maximum and mean absolute error voltage obtained during the validation is respectively 75 mV and 4 mV. Thus, battery model is defined (2), implemented in Matlab/Simulink and validated, where the model parameters R_{int} and OCV are respectively illustrated in Fig.10,11, during pulse charge/discharge phase. By the evaluation of internal resistance depicted in Fig.10, it's noticeable an increase of R_{int} at the extreme of SOC, while remains constant in the middle of SOC window. Moreover, internal resistance increases during the aging process. Considering the mean evaluated resistance of the new cell as 5.92 mΩ, the following internal mean resistance increase of the EOL cells are shown in Table III: it's evident an increase at least 200% of the internal resistance of the EOL cells respect to the fresh cell, but also, an increase of 470% of the cell at SOH=50% respect to the fresh cell and 200% of the cell at SOH=85%.

Results in Fig.11 depicts a noticeable difference between OCV discharge and charge curve due to hysteresis for NMC chemistry, in according to results shown in [16] for LiFePO4 based. As previously mentioned, in this paper the OCV value is evaluated as the battery voltage measured after 30 min of rest. Finally, an increase of OCV voltage curve during the aging process is observed, especially in charging phase. Thus an increase of the two RC-blocks resistance is observed, especially comparing the cell with SOH 100%, SOH ∈ [85,60]% and SOH=50%, as shown in Fig.12.

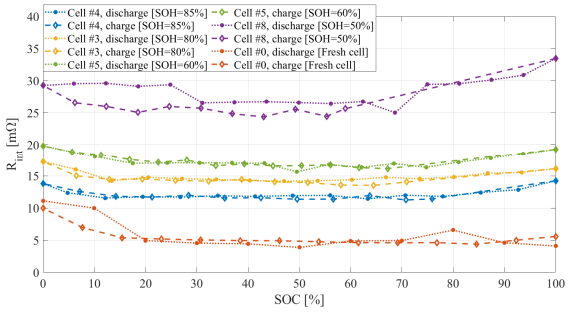

Fig. 10. Internal resistance evaluation of NMC cells at different SOH, during charging and discharging phase.

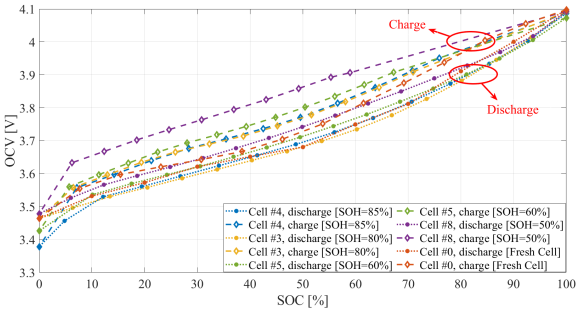

Fig. 11. Open Circuit Voltage evaluation of NMC cells at different SOH, during charging and discharging phase.

TABLE III. INCREASE OF INTERNAL RESISTANCE VS. STATE OF HEALTH

Cell n.	**#0**	**#4**	**#3**	**#5**	**#8**
SOH [%]	100	85	80	60	50
Mean R_{int} [mΩ]	5.92	12.08	14.72	17.35	27.81
R_{int} increase scale factor	1	2.04	2.49	2.93	4.70

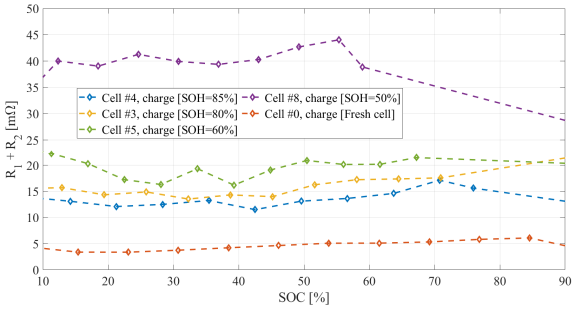

Fig. 12. Sum of RC-blocks resistance evaluation of NMC cells at different SOH, during charging phase.

V. CONCLUSIONS

This paper has shown NMC battery performance and voltage behavior considering the aging process.

In particular, authors investigated the battery performance after their EOL in automotive field, to understand if this battery could be re-used for stationary application, requiring low performance. The influence of temperature on battery performance is not considered in this paper.

The results have demonstrated that the coulombic efficiency of EOL batteries, respect to the fresh battery, strongly decrease when battery discharge C-Rate increases.

Finally, it's noticeable an increase of the battery internal resistance when battery capacity is decreasing. In particular there is a huge difference between battery at 60% and 50% of SOH.

By these last deductions, EOL batteries could be considered as energy storage for stationary applications, which require low performance, in terms of low charge/discharge current C-Rate, cycling the battery until the 60% of SOH.

ACKNOWLEDGMENT

The present work is using battery cells coming from the ENEA research center and the University of Pisa. Authors wish to thank all for their support and collaboration. All the activities reported in this paper were carried out within the Smart Energy Lab of the University of Florence.

REFERENCES

[1] Kocs, E. A. (2017). The global carbon nation: Status of CO2 capture, storage and utilization. In EPJ Web of Conferences (Vol. 148, p. 00002). EDP Sciences.

[2] Iclodean, C., Varga, B., Burnete, N., Cimerdean, D., & Jurchiș, B. (2017, October). Comparison of different battery types for electric vehicles. In IOP conference series: materials science and engineering (Vol. 252, No. 1, p. 012058). IOP Publishing.

[3] Martinez-Laserna, E., Gandiaga, I., Sarasketa-Zabala, E., Badeda, J., Stroe, D. I., Swierczynski, M., & Goikoetxea, A. (2018). Battery second life: Hype, hope or reality? A critical review of the state of the art. Renewable and Sustainable Energy Reviews, 93, 701-718.

[4] Lacey, G., Putrus, G., & Salim, A. (2013, July). The use of second life electric vehicle batteries for grid support. In Eurocon 2013 (pp. 1255-1261). IEEE.

[5] Bobba, S., Podias, A., Di Persio, F., Messagie, M., Tecchio, P., Cusenza, M. A., ... & Pfrang, A. (2018). Sustainability Assessment of Second Life Application of Automotive Batteries (SASLAB). JRC Exploratory Research (2016-2017), Final report.

[6] Locorotondo, E., Pugi, L., Berzi, L., Pierini, M., & Lutzemberger, G. (2018, June). Online identification of Thevenin equivalent circuit model parameters and estimation State Of Charge of Lithium-Ion batteries. In 2018 IEEE International Conference on Environment and Electrical Engineering and 2018 IEEE Industrial and Commercial Power Systems Europe (EEEIC/I&CPS Europe) (pp. 1-6). IEEE.

[7] Omar, N., Monem, M. A., Firouz, Y., Salminen, J., Smekens, J., Hegazy, O., ... & Van Mierlo, J. (2014). Lithium iron phosphate based battery–assessment of the aging parameters and development of cycle life model. Applied Energy, 113, 1575-1585.

[8] Lin, X., Stefanopoulou, A. G., Perez, H. E., Siegel, J. B., Li, Y., & Anderson, R. D. (2012, June). Quadruple adaptive observer of the core temperature in cylindrical Li-ion batteries and their health monitoring. In 2012 American Control Conference (ACC) (pp. 578-583). IEEE.

[9] Huria, T., Ludovici, G., & Lutzemberger, G. (2014). State of charge estimation of high power lithium iron phosphate cells. Journal of Power Sources, 249, 92-102.

[10] Kim, I. S. (2006). The novel state of charge estimation method for lithium battery using sliding mode observer. Journal of Power Sources, 163(1), 584-590.

[11] Waag, W., Fleischer, C., & Sauer, D. U. (2014). Critical review of the methods for monitoring of lithium-ion batteries in electric and hybrid vehicles. Journal of Power Sources, 258, 321-339.

[12] Jongerden, M. R., & Haverkort, B. R. (2009). Which battery model to use?. IET software, 3(6), 445-457.

[13] Ahmed, R., El Sayed, M., Arasaratnam, I., Tjong, J., & Habibi, S. (2014). Reduced-order electrochemical model parameters identification and soc estimation for healthy and aged li-ion batteries part i: Parameterization model development for healthy batteries. IEEE journal of emerging and selected topics in power electronics, 2(3), 659-677.

[14] D. Cittanti, A. Ferraris, A. Airale, S. Fiorot, S. Scavuzzo, and M. Carello, "Modeling Li-ion batteries for automotive application: A trade-off between accuracy and complexity," International Conference of Electrical and Electronic Technologies for Automotive, Torino 15-16 June 2017, pp.8,2017,ISBN:978-88-87237-26-9,DOI: 10.23919/EETA.2017.7993213.

[15] Ceraolo, M., Lutzemberger, G., Poli, D., & Scarpelli, C. (2019, June). Model parameters evaluation for NMC cells. In 2019 IEEE International Conference on Environment and Electrical Engineering and 2019 IEEE Industrial and Commercial Power Systems Europe (EEEIC/I&CPS Europe) (pp. 1-6). IEEE.

[16] Huria, T., Ludovici, G., & Lutzemberger, G. (2014). State of charge estimation of high power lithium iron phosphate cells. Journal of Power Sources, 249, 92-102.

[17] Zhang, C., Allafi, W., Dinh, Q., Ascencio, P., & Marco, J. (2018). Online estimation of battery equivalent circuit model parameters and state of charge using decoupled least squares technique. Energy, 142, 678-688.

[18] Eddahech, A., Briat, O., & Vinassa, J. M. (2015). Performance comparison of four lithium–ion battery technologies under calendar aging. Energy, 84, 542-550.

[19] Huria, T., Ceraolo, M., Gazzarri, J., & Jackey, R. (2012, March). High fidelity electrical model with thermal dependence for characterization and simulation of high power lithium battery cells. In 2012 IEEE International Electric Vehicle Conference (pp. 1-8). IEEE.

[20] Andrenacci, N., & Sglavo, V. (2017). Stato dell'arte dei modelli di invecchiamento per le celle litio-ione. Applicazione al caso di studio delle celle NMC invecchiate in ENEA. Report RDS/PAR2016/

[21] Ceraolo, M., Giglioli, R., Lutzemberger, G., Langroudi, M. M., Poli, D., Andrenacci, N., & Pasquali, M. (2018, June). Experimental analysis of NMC lithium cells aging for second life applications. In 2018 IEEE International Conference on Environment and Electrical Engineering and 2018 IEEE Industrial and Commercial Power Systems Europe (EEEIC/I&CPS Europe) (pp. 1-6). IEEE.